Polymer Journal, Vol. 39, No. 1, pp. 81–89 (2007)

Highly Transparent Photosensitive Polybenzoxazole: Poly(*o*-hydroxy amide) Derived from 4,4′-(Hexafluoroisopropylidene)bis(*o*-aminophenol) and *o*-Substituted Dicarboxylic Acid Chlorides

Yuji SHIBASAKI, Fumihiro TOYOKAWA, Shinji ANDO, and Mitsuru UEDA†

Department of Organic and Polymeric Materials, Graduate School of Science and Engineering, Tokyo Institute of Technology, 2-12-1-H120, O-okayama, Meguro-ku, Tokyo 152-8552, Japan

(Received September 15, 2006; Accepted November 1, 2006; Published December 7, 2006)

ABSTRACT: A novel poly(*o*-hydroxyamide) (PHA) as a precursor of photosensitive polybenzoxazole (PSPBO) that exhibits high transparency at 365 nm wavelength (*i*-line) has been developed. Time-dependent density functional theory (TD-DFT) calculations using the B3LYP hybrid functional were performed to predict the transparencies of various *o*-hydroxyamides in the *i*-line region. Based on these results, 2,2′-dimethyl-biphenyl-3,3′-dicarboxylic acid chloride was prepared and polymerized with 4,4′-(hexafluoroisopropylidene)bis(*o*-aminophenol). The resulting PHA-**3** showed a high transparency (92%, 1.0×10^{-3} mol/L in *N*,*N*-dimethylacetamide (DMAc)), superior to that of the conventional PHA-**1** (83% at the same concentration in DMAc) derived from 4,4′-oxybis(benzoyl chloride) in transparency. The positive-type PSPBO was then formulated based on PHA-**3** with a cross-linker 1,3,5-tris[(2-vinyloxy)ethoxy]-benzene (TVEB) and a photoacid generator (5-propylsulfonyloxyimino-5*H*-thiophen-2-ylidene)-2-(methylphenyl)-acetonitrile (PTMA), and the resulting polymer film (1.5 μm-thick) demonstrated the high photosensitivity and contrast of 32 mJ/cm^2 and 7.2, respectively. A clear positive image featuring 6 μm line-and-space was obtained, when a 6.0 μm-PSPBO film containing PHA-**3**, TVEB, and PTMA (15:3:2 in weight ratio) was exposed to *i*-line at 80 mJ/cm^2, post-baked at 120 °C for 5 min, developed with an alkaline tetramethylammonium hydroxide solution. The positive image was converted to the corresponding polybenzoxazole pattern upon heating at 350 °C. [doi:10.1295/polymj.PJ2006114]

KEY WORDS Optical Transparency / *o*-Hydroxybenzamide / Poyhydroxyamide / Density Functional Theory / Photosensitive Polybenzoxazole / Cross-linker / Photopatternable /

The thermal and dielectric characteristics of photosensitive polyimide (PSPI) are acceptable for a number of applications in the semiconductor industry, and a wide variety of PSPI has been developed and are made commercially available to meet requirements of different applications, such as inter-level insulation, stress buffer layer, and α-ray shielding layers of semiconductor devices.[1] PI, however, has numerous imide groups that increase water uptake and dielectric constant.[2] Polybenzoxazole (PBO) is known as an super engineering thermoplastics, and its properties are comparable with PI. In addition, the absence of carbonyl group in PBO results in lower water uptake and dielectric constant.[2] Thus, the photosensitive polybenzoxazole (PSPBO) is attracting great attention as substitute for conventional PSPI in recent years.[3–12]

The commercially available PSPBO is based on poly(*o*-hydroxy amide) (PHA), which is usually prepared by polycondensation of 4,4′-(hexafluoroisopropylidene)bis(*o*-aminophenol) (**12**) and 4,4′-oxybis-(benzoic acid) (**8a**) using a condensation agent, because of its high transparency at 365 nm wavelength (*i*-line).[13,14] There is an increasing demand for thicker films for small package to act as a buffer layer and α-ray shielding applications,[15,16] consequently, it is quite important to develop a novel photosensitive polymer with higher transparency for UV lithography. The absorption of PI and PBO in *i*-line region corresponds to the excitation of electrons such as transitions involving *p*, *s*, and *n* electrons, charge-transfer (CT) electrons, and *d* and *f* electrons. Recently, we have demonstrated that the time-dependent density functional theory (TD-DFT) calculations using the B3LYP hybrid functional with the 6-311++G(d,p) basis set can well reproduce UV spectra in the measurements of model compounds without incorporation of empirical corrections.[17] Utilizing this method, the absorption in *i*-line region of the above mentioned PHA was found to be the CT type transition between the benzoic acid and the *o*-hydroxyamide rings. Therefore, we designed and prepared a novel transparent PSPBO based on 4,4′-sulfonylbis(*o*-aminophenol) (**13**) and 4,4′-oxybis(benzoyl chloride) (**8b**) for *i*-line lithography.[18] Introduction of a sulfone group as a substitute for hexafluoroisopropylidene group is effective to lower the HOMO levels, and thus increases

†To whom correspondence should be addressed (E-mail: mueda@polymer.titech.ac.jp).

the band gaps, which causes hypochromic (blue) shifts of the absorptions originating from the HOMO → LUMO transitions.

We here describe the design and synthesis of a novel PSPBO with higher transparency at 365 nm wavelength based on **12** as one of the monomers. The structure of PBO precursor is designed to prevent the CT transition using the prediction of our calculation method. Thus, 3,3′-bis(2-methylbenzoyl chloride) (**9b**) or 2,4-dimethylterephthaloyl chloride (**10b**) as a bis(carboxylic acid) derivative and **12** as a bis(*o*-hydroxyamine) are used as monomers, and a novel PSPBO for *i*-line lithography is formulated using 1,3,5-tris-[(2-vinyloxy)ethoxy]benzene (TVEB)[19] as an acidolytic de-cross-linker, and (5-propylsulfonyloxyimino-5*H*-thiophen-2-ylidene)-(2-methylphenyl) acetonitrile (PTMA)[20] as a photoacid generator in conjunction with the preparing PHA.

EXPERIMENTAL

Materials

o-Hydroxybenzamides, 2-hydroxybenzanilide (**1**),[21] 2-methyl-2′-hydroxybenzanilide (**2**),[22] and 2-benzamidophenyl benzoate (**6**)[23] were prepared according to the literature. Bis(*o*-hydroxyamide)s **12** and **13** were prepared according to the literature.[18] Compounds **8a** and **10a** were purchased from TCI Organic Chemicals and used as received. PHAs were prepared by polycondensation of diacid chlorides and bis(*o*-aminophenol)s in the presence of LiCl as an additive. 1-Methyl-2-pyrrolidinone (NMP) was purified by vacuum distillation from calcium hydride and stored over 4 Å molecular sieves. Tetrahydrofuran (THF) was purified by distillation from sodium metal and benzophenone. Zinc powder is washed with 1 mol/L hydrochloric acid and ethanol, dried at 100 °C *in vacuo* for 2 h. PTMA and TVEB were kindly donated from Ciba specialty and Tokyo Ohka Kogyo Co. Ltd, respectively, and used as received. Other reagents and solvents were used as received.

Model Compounds

The following model compounds were prepared from the corresponding acid chlorides and amines according to the literature.

Compound **1**. 85% yield. mp 175–176 °C (lit.[21] 170–171 °C).

Compound **2**. 82% yield. mp 182–187 °C (lit.[22] 182–183 °C).

2-Methoxy-2′-Hydroxybenzanilide (**4**). 90% yield. mp 203–206 °C. *Anal.* Calcd for $C_{14}H_{13}N_1O_3$: C, 69.12%; H, 5.39%; N, 5.79%; Found: C, 69.84%; H, 5.60%; N, 5.74%.

2,6-Dimethoxy-2′-Hydroxybenzanilide (**5**). 75% yield. mp 210–214 °C. *Anal.* Calcd for $C_{15}H_{15}N_1O_4$: C, 65.92%; H, 5.53%; N, 5.13%; Found: C, 66.64%; H, 5.64%; N, 4.70%.

2-Benzamidophenyl Benzoate (**6**). 91% yield. mp 262–263 °C (lit.[21] 264 °C).

*Synthesis of 2-Methyl-3-Chlorobenzoic Acid Methylester (**7**)*

The title compound was prepared according to the literature.[23] Thus, to a solution of 3-chloro-2-methyl benzoic acid (10.0 g, 58.8 mmol) in methanol (100 mL) was added several drops of concentrated sulfuric acid. The mixture was refluxed for 24 h, cooled to room temperature, and evaporated under the reduced pressure. The residue was poured into water, and the precipitate was collected, washed with water, and dried *in vacuo* at 50 °C over P_2O_5. Recrystallization from methanol and water (1:4 in volume) gave white crystals. The yield was 10.2 g (94%). mp 34 °C (lit.[24] 16.5 °C).

*Synthesis of 2,2′-Dimethyl-Biphenyl-3,3′-Dicarboxylic Acid (**9a**)*

To a solution of tetraethylammonium iodide (1.5 g, 6.0 mmol) in THF (50 mL) was added bis(triphenylphosphine)nickel(II) dicloride (2.13 g 3.20 mmol) and zinc powder (2.45 g 37.5 mmol) under nitrogen. The mixture was kept stirring for 30 min at 25 °C, and then **7** (4.50 g, 24.4 mmol) was added. The mixture was stirring for 20 h at 50 °C, and the resulting solution was filtered, and evaporated. The residue was dissolved in EtOH (50 mL) and KOH (6.8 g 123.6 mmol) was added. The mixture was refluxed for 7 h, cooled to room temperature, and 1 N HClaq was added until the pH value became about 1. The precipitate was collected, washed with water, and dried *in vacuo* at 50 °C over P_2O_5. Recrystallization from methanol gave white crystals. The yield was 2.2 g (67%). mp 279–282 °C. IR (KBr, cm^{-1}): 3300–3000 (O–H), 1681 (C=O). ^1H NMR (300 MHz, DMSO-d_6, δ, ppm): 7.79 (dd, 2H, ArH), 7.36 (t, 2H, ArH), 7.25 (dd, 2H, ArH) 2.15 (s, 6H, $-CH_3$). *Anal.* Calcd for $C_{16}H_{14}O_4$: C, 71.10%; H, 5.22%; O, 23.68%; Found: C, 71.51%; H, 5.37%; O, 23.12%.

*Synthesis of 2,4,6-Trimethylisophthalic Acid (**11a**)*

Into a flask containing KOH (7.3 g, 130 mmol) and water (250 mL) was added 2,4-bis(chloromethyl)-1,3,5-trimethylbenzene (6.5 g, 32.5 mmol), and the mixture was refluxed for 24 h. The solution was cooled to room temperature, and $KMnO_4$ (2.1 g, 13.2 mmol) was carefully added. After 12 h, the solution was filtered to remove inorganic salts, and acidified with HClaq. The precipitate was washed with water and dried under reduced pressure at 50 °C for 12 h.

The yield was 5.8 g (86%). ^{1}H NMR (300 MHz, DMSO-d_6, δ, ppm): 6.83 (s, 1H, ArH), 2.31 (s, 3H, –CH_3), 2.27 (s, 6H, –CH_3). *Anal.* Calcd for $C_{11}H_{12}O_4$: C, 63.45%; H, 5.81%; O, 30.74%; Found: C, 63.49%; H, 5.90%; O, 30.68%.

Diacid Chlorides

The following diacids chlorides were prepared by refluxing the corresponding diacids in $SOCl_2$, and recrystallized from hexane.

Compound **8b** 66% yield. mp 83–84 °C (lit.[18] 91 °C).

3,3′-Bis(2-methylbenzoylchloride) (**9b**) 58% yield. mp 74–75 °C. *Anal.* Calcd for $C_{16}H_{14}O_4$: C, 71.10%; H, 5.22%; O, 23.68%; Found: C, 71.19%; H, 5.29%; O, 23.62%.

2,5-Dimethylterephthaloyl Dichloride (**10b**) 64% yield. mp 118–119 °C (lit.[24] 120–121 °C).

2,4,6-Trimethylisophthaloyl Dichloride (**11b**) 62% yield. bp 60 °C/9 mmHg. *Anal.* Calcd for $C_{11}H_{10}Cl_2O_2$: C, 53.90%; H, 4.11%; O, 13.06%; Found: C, 53.85%; H, 4.07%; O, 13.10%.

Polymerization

Typical polymerization procedure is as follows: To a solution of **13** (733 mg, 2.00 mmol) and LiCl (216 mg 5.1 mmol) in NMP (10 mL) was added dropwise **9** (540 mg, 2.00 mmol) at 0 °C. Polymerization was kept at that temperature for 30 min, and then at 25 °C for 24 h. The resulting viscous solution was poured into methanol and water (vol % 1:1), and the precipitate was filtered and dried at 100 °C under reduced pressure, giving white powder.

*PHA-**3*** The yield was 1.18 g (99%): M_n and M_w/M_n: 8000 and 1.9 (determined by GPC (DMF, PSt standards)). IR (film) = 3413 (O–H stretching) and 1654 (NHC=O stretching) cm^{-1}. ^{1}H NMR (DMSO-d_6) = 10.33 (s, 2H –OH), 9.65 (s, 2H amide) 8.07 (s, 2H) 7,60 (d, 2H) 7.43 (t, 2H) 7.26 (d, 4H) 7.06 (s, 2H) 2.16 (s, 6H) ppm. *Anal.* Calcd for $C_{31}H_{22}F_6N_2O_4$: C, 62.00%; H, 3.69%; N, 4.66%; Found: C, 61.95%; H, 4.66%; N, 4.76%.

*PHA-**4*** The yield was 1.04 g (99%): M_n and M_w/M_n: 11000 and 2.1 (determined by GPC (DMF, PSt standards)). IR (film) = 3424 (O–H stretching) and 1654 (NHC=O stretching) cm^{-1}. ^{1}H NMR (DMSO-d_6) = 10.29 (s, 2H –OH), 9.43 (s, 2H amide) 8.00 (s, 2H) 7,46 (s, 2H) 7.00 (s, 2H) 2.51 (s, 6H) ppm. *Anal.* Calcd for $C_{25}H_{18}F_6N_2O_4$: C, 57.26%; H, 3.46%; N, 5.34%; Found: C, 56.35%; H, 4.29%; N, 6.17%.

*PHA-**5*** (containing ester) The yield was 1.04 g (55%): M_n and M_w/M_n: 6800 and 1.8 (determined by GPC (DMF, PSt standards)). IR (film) = 3448 (O–H stretching) and 1751 (OC=O stretching) 1640–1670 (NHC=O stretching) cm^{-1}.

*PHA-**6**(tert-BOC Functionalized PHA)*

Into a flask containing PHA-**1** (0.295 g, 0.526 mmol/unit) in NMP (3 mL) were added di-*tert*-butyldicarbonate (0.230 g, 1.06 mmol) and 4-*N*,*N*-dimethylpyridine (0.13 g, 1.06 mmol) at 25 °C. After 2 h, the solution was poured into water, and precipitate was collected, dried under reduced pressure at 50 °C to give white powder. The yield was 0.280 g (75%): M_n and M_w/M_n: 30000 and 1.7 (determined by GPC (DMF, PSt standards)). IR (film) = 1751 (OC=O stretching) 1654 (NHC=O stretching) cm^{-1} *Anal.* Calcd for $C_{39}H_{34}F_6N_2O_9$: C, 59.39%; H, 4.35%, N, 3.35%; Found: C, 59.21%; H, 4.66%, N, 3.39%.

Dissolution Rate

All baking processes were performed on a hot plate with a digital thermo-controller. TVEB (5–15 wt % to PHA) and PTMA (1–5 wt % to PHA) were dissolved in PHA solution in DMAc (20 wt % of PHA) to construct a photosensitive polymer. The polymer film spin-cast on a silicon wafer was prebaked (PB) at 80–130 °C for 5 min, exposed to a filtered super-high-pressure mercury lamp at *i*-line, post exposure baked (PEB) at 100–130 °C for 5 min, and developed with a 2.38 wt % tetramethylammonium hydroxide aqueous solution (TMAHaq) at 25 °C. The changes in the film thickness to TVEB, PTMA, and baking temperatures were measured with a Dektak^3 surface profiler.

Photosensitivity

A 3 μm thick polymer film on a silicon wafer was PB at 120 °C for 5 min, exposed to *i*-line, PEB at 120 °C for 5 min, and developed with 2.38 wt % TMAHaq at 25 °C. A characteristic curve was obtained by plotting a normalized film thickness against exposure energy. The image exposure was obtained as a contact print.

Measurements

Infrared (IR) spectra were recorded on a Horiba FT-210 spectrophotometer. Ultraviolet-visible (UV-vis) spectra were obtained on a Jasco V-560 spectrophotometer. Number- and weight-average molecular weights (M_n and M_w) were determined by a gel permeation chromatography (GPC) with polystyrene calibration using Tosoh HLC-8120 system equipped with polystyrene gel columns (TSK GELs, GMH_{HR}-M and GMH_{HR}-L) at 40 °C in DMF (containing 0.01 M of lithium bromide, the flow rate: 1.0 mL min^{-1}). Film thickness was measured by a Dektak^3 surface profiler (Veeco Instrument Inc). The scanning electron microscope (SEM) photos were taken with a Technex Lab Tiny SEM 1540 scanning electron microscope with 15 kV accelerating voltage for imaging.

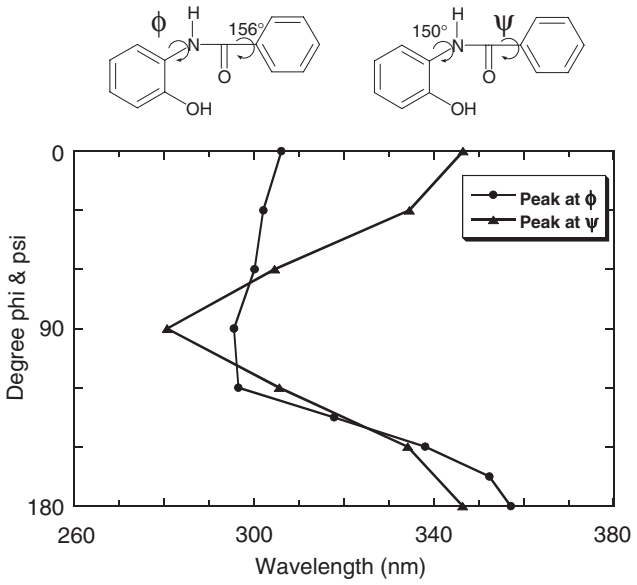

Figure 1. Calculated λ_{max} against dihedral angles of **1**.

RESULTS AND DISCUSSION

Prediction of UV Absorption around 365 nm Wavelength of o-Hydroxyamide Derivatives

In a previous paper,[18] the absorption in *i*-line region of PHA was found to be the CT type transition between the benzoic acid and the *o*-hydroxybenzamide rings, and UV absorptions of *o*-hydroxybenzamide and PHA were well reproduced by the TD-DFT theory using the B3LYP hybrid functional with the 6-311++G (d, p) basis set. Using this calculation, the effect of dihedral angles of ϕ (between *o*-hydroxybenzene and amide planes) and Ψ (between benzene and amide planes) in **1** on the maximum UV absorption (λ_{max}) is illustrated in Figure 1. The λ_{max} value for Ψ decreases continually from 345 nm at 0°, shows a minimum of 280 nm at 90°, and then increases to 345 nm at 180°. On the other hand, after a little decrease from 305 nm at 0° to 295 nm at 90°, the λ_{max} value for ϕ increases more rapidly to 355 nm at 180°. These indicate that increasing dihedral angles decreases HOMO level and increases LUMO level, resulting in large band-gap (blue shift). Moreover, in the case of the angle ϕ, the band-gap energy is also related to hydrogen bonding between hydroxyl and carbonyl moieties. The structure of *o*-hydroxybenzamide to have the optimum energy was determined by our calculation method, in which the angles ϕ and Ψ were calculated to be 150° and 156°, respectively. Based on the calculation described above, to shift the λ_{max} value into shorter wavelength, introduction of substituents on *ortho* position of amide group is effective. Thus, several *o*-hydroxybenzamide derivatives were investigated by our calculation to predict their absorbance in *i*-line region.

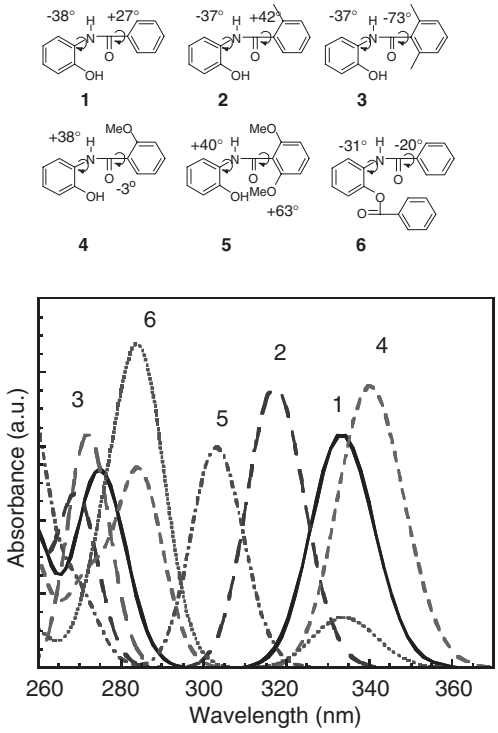

Figure 2. Calculated UV-vis spectra of *o*-hydroxybenzamides.

Figure 2 depicts the dihedral angles on optimum energy, and variation of calculated absorbance with wavelength of UV light for various *o*-hydroxybenzamides **1**–**6**. As our prediction, introduction of substituents such as methyl (**2**), dimethyl (**3**), and dimethoxy (**5**) groups effectively increases the dihedral angles of Ψ, and lower the λ_{max} values from 333 nm to 315, 270, and 303 nm, respectively. On the other hand, incorporation of monomethoxy unit (**4**) decreases the value of Ψ and thus increases the λ_{max} values from 333 nm to 340 nm. This may be explained by the formation of hydrogen bonding between amide proton and methoxy oxygen. The λ_{max} of CT transition of **6** is observed at 283 nm, which indicates scission of hydrogen bonding and introduction of substituents on *ortho* position are efficient to lower λ_{max} values.

Synthesis of Various o-Hydroxyamides, Their UV Aborptions

Figure 3 depicts the observed transmittance of *o*-hydroxybenzamide, **1**, **2**, **4**, **5**, and **6**, which were prepared by selective amidation of *o*-aminophenol with the corresponding benzoyl chlorides in the presence of LiCl. Non-substituted *o*-hydroxybenzamide **1** absorbs the light above 320 nm, thus opaque at *i*-line. Introduction of substituents is effective to twist the conjugated planes, resulting in increasing band-gap energy and increasing transmittance at *i*-line. In addi-

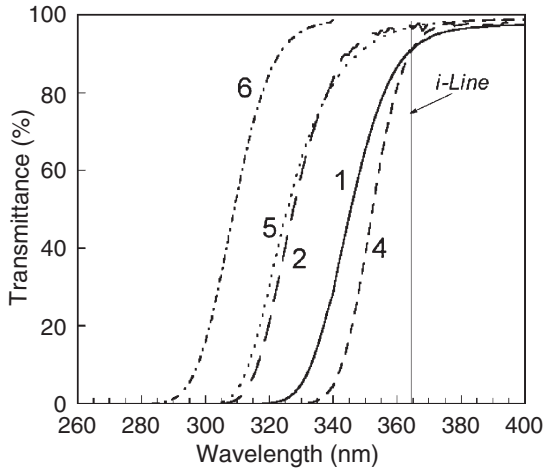

Figure 3. UV-vis spectra of *o*-hydroxybenzamides in DMAc (1.0×10^{-3} mol/L).

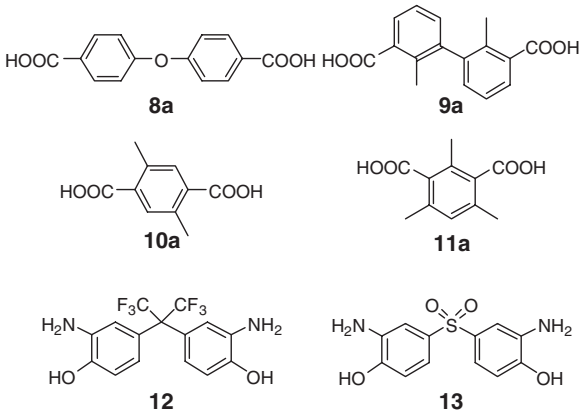

Figure 4. Dicarboxylic acid chlorides and bis(*o*-hydroxybenzamide)s for transparent PHA.

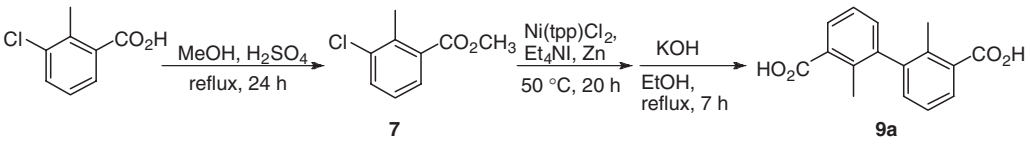

Scheme 1.

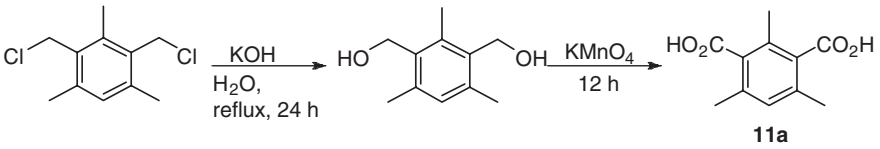

Scheme 2.

tion, depending on the substituents the transmittance of the substitutes is different, and the order of the transparency was **4** < **1** < **2** < **5** < **6**, which were well predicted by our MO calculations in Figure 2. Therefore, we chose dicarboxylic acid derivatives **8**–**11** as a comonomer of diamines **12** and **13** (Figure 4).

Synthesis of Dicarboxylic Acid Chlorides, PHAs, and Their UV-Absorption

Based on the preliminary study, we designed comonomers **8b**–**11b**, which were prepared by refluxing the corresponding dicarboxylic acids in thionyl chloride, followed by recrystallization from hexane in moderate yield (58–64%). Compound **9a** was prepared from 3-chloro-2-methylbenzoic acid, followed by esterification, cross-coupling reaction using Ni catalyst, and alkaline hydrolysis of the ester (Scheme 1). Compound **11a** was prepared from 2,4-bis(chloromethyl)-1,3-5-trimethylbenzene, followed by alkaline hydrolysis, and oxidation as shown in Scheme 2. Using these comonomers, PHAs were prepared by conventional polycondensation in the presence of LiCl as an additive (Scheme 3, runs **1**–**5** in Table I). All the polymers except for that from **12** and **11b** (PHA-**5**) were obtained in excellent yield, and showed characteristic amide absorptions at 1654 cm^{-1}, and no absorption was observed at 1743 cm^{-1} corresponding to ester carbonyl stretching in IR spectra. PHA-**5** obtained from **12** and **11b** contains ester linkage as well as desired amide bond, suggesting esterification partially occurred during polycondensation. The molecular weights of PHA-**3**, **4**, **5** from comonomers **9b**–**11b** were not high (runs **3**–**5**) compared to PHA-**1**,**2** from comonomer **8b**, probably due to the steric hindrance of **9b**–**11b**. The molecular weights of these polymers were over 7,000, and the films were transparent and colored slightly yellow, indicating these can be applicable to photosensitive polymer.

Figure 5 depicts the transmittance of prepared PHA-**1**–**5** and PHA-**6** in DMAc (1 mmol/L unit), which was obtained by condensation of PHA-**1** with di-*tert*-butyldicarbonate. While the conventional PHA (PHA-**1**) shows 82% transparency at *i*-line, all the prepared PHAs show better transparency. The transparen-

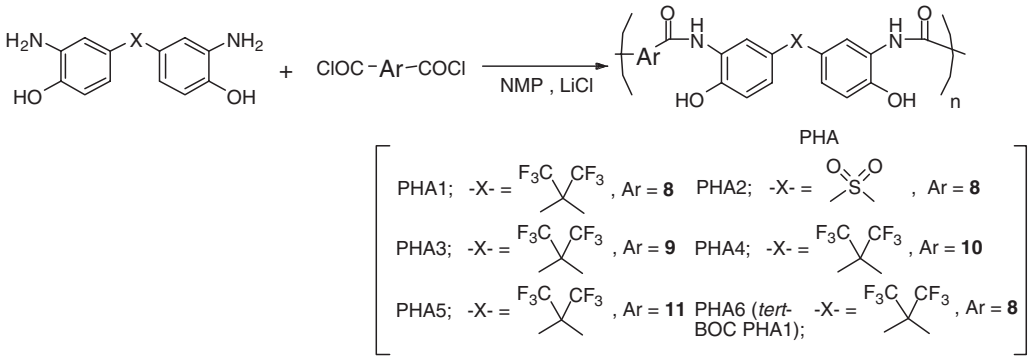

Scheme 3.

Table I. PHA synthesis

PHA	Bis(*o*-aminophenol)	Diacid chloride	Yield	M_n[a]	M_w/M_n[a]
1	**12**	**8b**	93	25000	1.6
2	**13**	**8b**	92	28000	2.4
3	**12**	**9b**	99	8000	2.1
4	**12**	**10b**	98	11000	2.2
5[b]	**12**	**11b**	55	6800	1.7

[a]Determined by GPC (PSt, DMF). [b]Containing ester in the main chain.

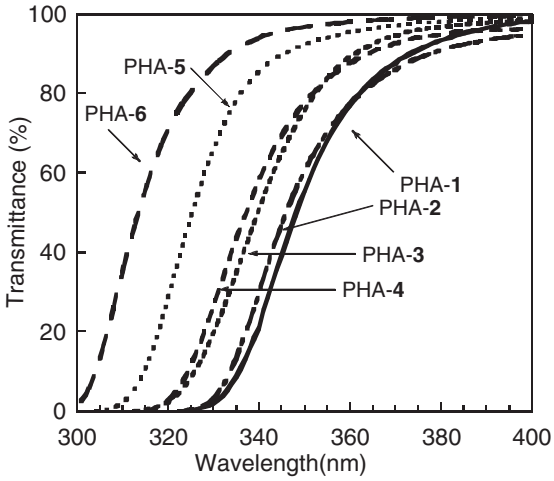

Figure 5. Transparency of PHAs in DMAc (1.0×10^{-3} mol/L).

cy of the PHAs is in the order of PHA-**1**, **2** < **3**, **4** < **5** < **6**, which are well agreed with the transparency of model compounds. Especially, PHA-**3**–**6** show excellent transparency over 90%, however, PHA-**5** contained a ester linkage in the backbone. To make a photosensitive polymer film using the system described in our previous paper,[18] an alkaline developable group –OH should be in a polymer chain, thus PHA-**5** and PHA-**6** were not suitable for this purpose. However, there can be little doubt that PHA-**6** is still a good candidate to make a transparent photosensitive PBO film if it was mixed with a photoacid generator. Considering the solubility and film formation property, PHA-**3** was selected as an alkaline developable matrix for the PSPBO.

*Photopatterning of PHA-**3** Based Photosensitive Polymer Using Cross-Linker and PAG*

The PSPBO was then formulated with PHA-**3**, TVEB, and PTMA for *i*-line lithography. A positive-tone pattern formation mechanism is described in a previous report.[18] Thus, the photosensitive polymer film was produced by spin-cast a resist solution, followed by thermal treatment (PB) to promote the cross-linking between PHA-**3** with TVEB *via* acetal linkage. Irradiation with *i*-line causes degradation of PTMA, producing a sulfonic acid that promotes scission of acetal linkage between PHA-**3**, resulting in the alkaline developable film. To obtain high resolution and contrast, the effects of PB and PEB temperatures, and amounts of TVEB and PTMA loadings were investigated.

PHA-**3** and TVEB were dissolved in DMAc (PHA content 20 wt %), and the solution was spin-cast on a silicon wafer to obtain a 1.7 μm thickness polymer film. TVEB (15 wt % to PHA) was loaded and the film was PB for 5 min. Increasing the PB temperature, the cross-linking reaction of PHA with TVEB proceeded, finally (at 110 °C) resulting in the insoluble film with an alkaline developer as shown in Figure 6. TVEB loading was also effective to promote cross-linking reaction within the film. Thus, TVEB (0–15 wt %) was dissolved in PHA-**3** (20 wt % in DMAc), and the spin-cast film was prebaked at 120 °C for 5 min, and developed with a 2.38 wt % TMAHaq solution at 25 °C. As shown in Figure 7, the dissolution rate gradually decreases with increasing the amounts of TVEB. The film was almost insoluble in the developer at 15 wt % loading of TVEB. PTMA was then added as a film component to formulate the PSPBO film. For the effective decross-linking reaction of the film with

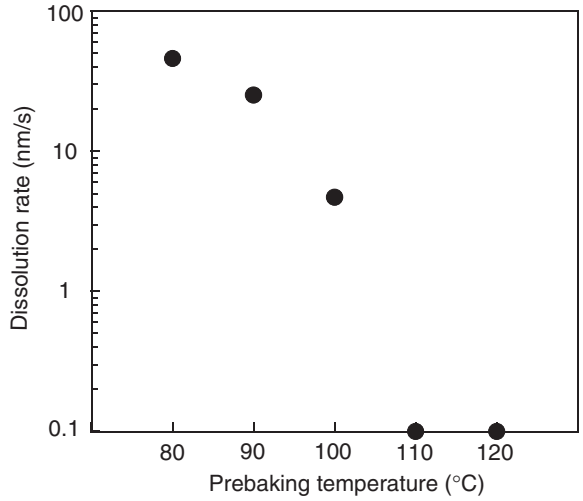

Figure 6. Effect of PB temperature on dissolution rate. Conditions; PHA-**3**, TVEB (15 wt % to PHA) in DMAc (20 wt % of PHA), PB for 5 min, 2.38 wt % TMAH solution at 25 °C as a developer.

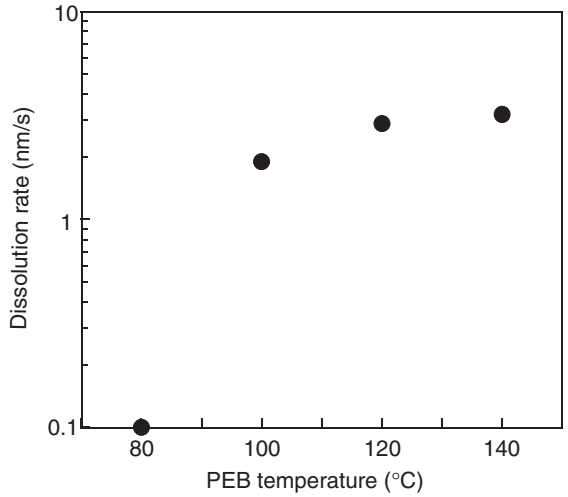

Figure 8. Effect of PEB temperature on dissolution rate. Conditions; PHA-**3**, TVEB (15 wt %), PTMA (10 wt %) in DMAc (20 wt % of PHA), PB at 120 °C for 5 min, *i*-line exposure at 100 mJ/cm^2, PEB for 5 min, 2.38 wt % TMAH solution at 25 °C as a developer.

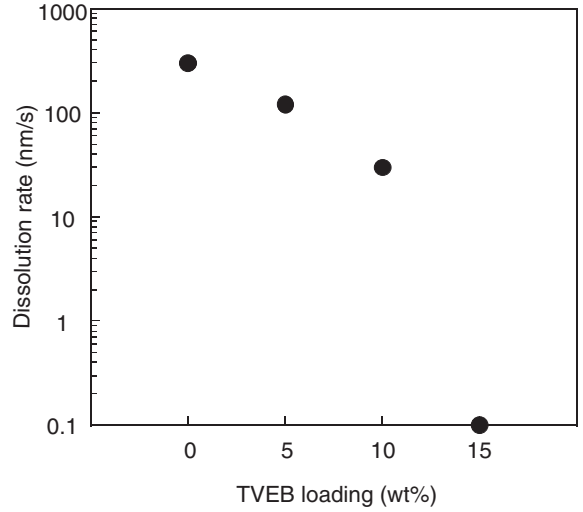

Figure 7. Relationship between dissolution rate and TVEB loading. Conditions; PHA-**3**, TVEB (0–15 wt %) in DMAc (20 wt % of PHA), PB at 120 °C for 5 min, 2.38 wt % TMAH solution at 25 °C as a developer.

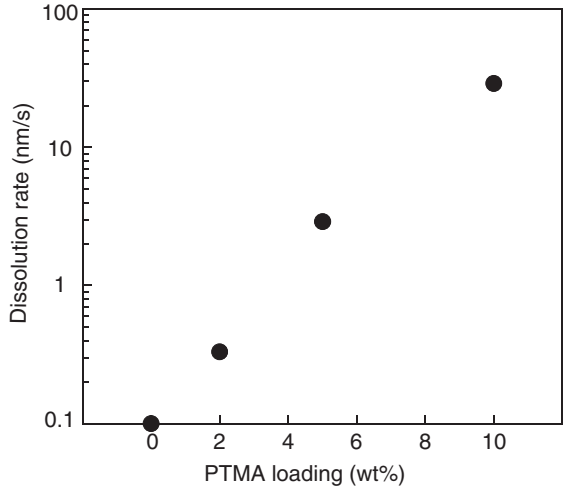

Figure 9. Effect of PTMA loading on dissolution rate. Conditions; PHA-**3**, TVEB (15 wt %), PTMA in DMAc (20 wt % of PHA), PB at 120 °C for 5 min, *i*-line exposure at 100 mJ/cm^2, PEB at 120 °C for 5 min, 2.38 wt % TMAH solution at 25 °C as a developer.

PTMA, the PEB temperature to diffuse the generated acid within the film and the amounts of this reagent are critical. Figure 8 depicts the effect of PEB temperature on dissolution rate of the photosensitive film. The film was prepared by spin-casting the PHA-**3** solution containing 15 wt % of TVEB and 10 wt % of PTMA, prebaked at 120 °C for 5 min, exposed with 365 nm light at 100 mJ cm^{-2}, PEB at 80–140 °C for 5 min, developed with a 2.38 wt % TMAHaq solution at 25 °C. The dissolution rate dramatically increases at 100 °C, from which becomes slow increase up to 140 °C. These results indicate that PEB treatment promoted the diffusion of the photo-generated acid in the film, accelerating the decross-linking reaction.

Figure 9 illustrates the relationship between the dissolution rate of the exposed film and the amounts of PTMA. Decreasing the amounts of PTMA decreased the dissolution rate, thus at least 10 wt % PTMA was required to obtain a good dissolution contrast.

Based on the above experimental results, the PSPBO was made by PHA-**3**, TVEB (15 wt %), and PTMA (10 wt %) in DMAC (PHA 20 wt %), spin-cast on a silicon wafer (film thickness 3 μm), PB at 120 °C for 5 min, exposed with *i*-line, PEB at 120 °C for 5 min, developed with TMAHaq at 25 °C to make photosensitive curve. From the minimum dose of *i*-

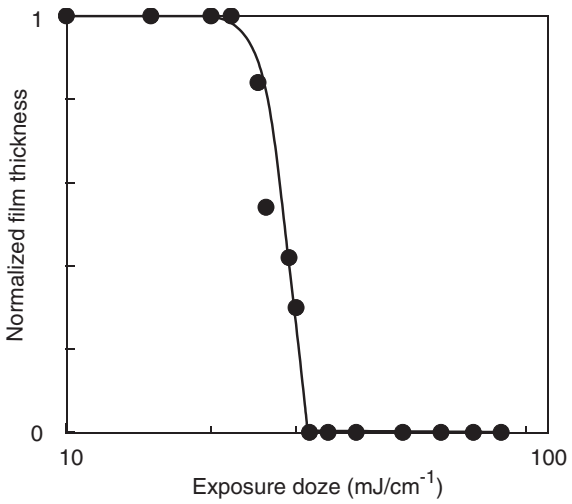

Figure 10. Photosensitivity curves of PHA-**3** based photosensitive polymers. Conditions; PHA, TVEB (15 wt %), PTMA (10 wt %) in DMAc (20 wt % of PHA), PB at 120 °C for 5 min, *i*-line exposure at, PEB at 120 °C for 5 min, 2.38 wt % TMAH solution at 25 °C as a developer.

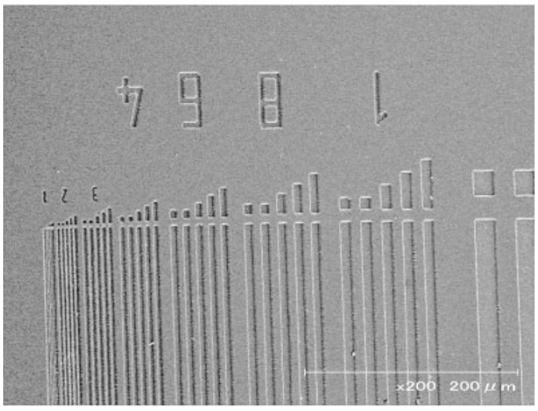

Figure 11. A representative SEM image of PSPBO film (3 μm thickness) derived from PHA-**3**.

line and the slope in Figure 10, the sensitivity and contrast of this PSPBO was determined to be 32 mJ/cm^2 and 7.2, respectively. Thus, the photo patterning was performed with *i*-line exposure at 80 mJ/cm^2 using above-mentioned conditions. The clear positive-tone image featuring 6 μm line and space was obtained as shown in Figure 11, and this image was almost maintained even after the film was cured consecutively for 1 h at each temperature 250, 300, and 350 °C to make the patterned PBO film (Figure 12).

CONCLUSIONS

Time-dependent density functional theory (TD-DFT) calculations using the B3LYP hybrid functional were found to be useful to predict the transparencies of various *o*-hydroxybenzamides in the *i*-line region.

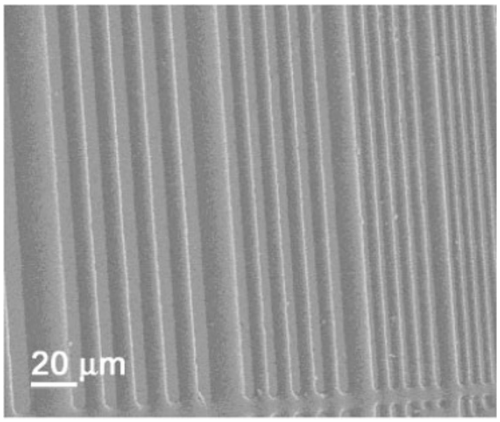

Figure 12. A representative SEM image of PSPBO film (3 μm thickness) derived from PHA-**3** cured consecutively for 1 h at each temperature, 250, 300, and 350 °C.

The absorbance of *o*-hydroxybenzamide at *i*-line region was revealed that the CT transition of aminophenol (HOMO) to benzoic acid units (LUMO). The band-gap energy of it was related to the dihedral angles between these two benzene rings, which were confirmed by the UV absorption of several *o*-hydroxybenzamides prepared by condensation of *o*-aminophenol with benzoic acid derivatives. Thus, PHAs were prepared by the conventional polycondensation in the presence of LiCl as an additive, and their transmittance at *i*-line were found in the order of the model compounds. One of the transparent PHA prepared in this study was applied to a photosensitive polymer matrix. The novel PSPBO consisting of PHA-**3**, TVEB, and PTMA showed the high photosensitivity and contrast. A positive image featuring 6 μm line and space was obtained by the contact printed image of the PHA-**3** film after alkaline development, and it was successfully converted to the corresponded PBO image by thermal treatment.

REFERENCES

1. "Polyimides Fundamentals and Applications," M. K. Ghosh and K. L. Mittal, Ed., Marcel Decker, New York, 1996.
2. G. Maier, *Prog. Polym. Sci.*, **26**, 3 (2001).
3. D. N. Khanna and W. H. Mueller, *Polym. Eng. Sci.*, **29**, 954 (1989).
4. T. Yamaoka, N. Nakajima, and K. Koseki, *J. Polym. Sci., Part A: Polym. Chem.*, **28**, 2517 (1990).
5. M. Ueda, K. Ebara, and Y. Shibasaki, *J. Photopolym. Sci. Technol.*, **16**, 237 (2003).
6. K. Ebara, Y. Shibasaki, and M. Ueda, *J. Photopolym. Sci. Technol.*, **16**, 287 (2003).
7. K. Ebara, Y. Shibasaki, and M, Ueda, *Polymer*, **44**, 333 (2003).
8. K. Fukukawa, Y. Shibasaki, and M. Ueda, *Polym. J.*, **36**, 489 (2004).
9. K. Fukukawa, Y. Shibasaki, and M. Ueda, *Polym. J.*, **37**, 74

(2005).
10. F. Toyokawa, Y. Shibasaki, and M. Ueda, *Polym. J.*, **37**, 517 (2005).
11. C. S. Hong, M. Jikei, R. Kikuchi, and M. Kakimoto, *Macromolecules*, **36**, 3174 (2003).
12. K. Fukukawa and M. Ueda, *Polym. J.*, **38**, 405 (2006).
13. M. D. Houtz, J. M. Lavoie, D. L. Pedrick, E. G. Jones, M. R. Unroe, and L. S. Tan, *Polym. Prepr., (Am. Chem. Soc., Div. Polym. Chem.)*, **35**, 437 (1994).
14. W. D. Joseph, J. C. Abed, T. H. Yoon, and J. E. McGrath, *Polym. Prepr., (Am. Chem. Soc., Div. Polym. Chem.)*, **35**, 551 (1994).
15. M.-S. Jung, S. K. Lee, H. J. Lee, M. K. Park, and H.-T. Jung, *J. Polym. Sci., Part A: Polym. Chem.*, **43**, 5520 (2005).
16. R. Rubner, *J. Photopolym. Sci. Technol.*, **17**, 685 (2004).
17. S. Ando, T. Fujigaya, and M. Ueda, *Jpn. J. Appl. Phys.*, **41,** **2A**, L105 (2002).
18. F. Toyokawa, K. Fukukawa, Y. Shibasaki, S. Ando, and M. Ueda, *J. Polym. Sci., Part A: Polym. Chem.*, **43**, 2527 (2005).
19. S.-Y. Moon, K. Kamenosono, S. Kondo, A. Umahara, and T. Yamaoka, *Chem. Mater.*, **6**, 1854 (1994).
20. T. Asakura, H. Yamato, A. Matsumoto, P. Murer, and M. Ohwa, *J. Photopolym. Sci. Technol.*, **16**, 335 (2003).
21. H. Seino, K. Iguchi, O. Haba, Y. Oba, and M. Ueda, *Polym. J.*, **31**, 822 (1999).
22. S. Vickers, D. J. Triggle, and D. R. Garrison, *J. Chem. Soc. [Section] C: Organic*, **6**, 632 (1968).
23. D. Peltier, *Bull. Soc. Scient. Bret.*, **31**, 7 (1956).
24. M. Ueda, Mitsuru, A. Takabayashi, and H. Seino, *Macromolecules*, **30**, 363 (1997).